Eddy currents in rectangular conductors: Analytical 2D loss model in the context of magnetic component design

Author(s):
Ewald, Thomas; Biela, Jürgen

Publication date:
2023

Permanent link:
https://doi.org/10.3929/ethz-b-000635633

Originally published in:
https://doi.org/10.23919/epe23ecceeurope58414.2023.10264392

Eddy currents in rectangular conductors: Analytical 2D loss model in the context of magnetic component design

Thomas Ewald, Jürgen Biela
SWISS FEDERAL INSTITUTE OF TECHNOLOGY
Rämistrasse 101, 8092
Zürich, Switzerland
Tel.: +41 / (44) 632.09.84
E-Mail: tewald@ethz.ch, jbiela@ethz.ch

URL: https://hpe.ee.ethz.ch/

ACKNOWLEDGEMENT

This research is financially supported by the Swiss Innovation Agency (Innosuisse) and the Bächli AG, Empowering Transformation. Application no.: 32328.1 IP-ENG

***Index Terms*—Power losses, Analytical losses computation, High-frequency windings, Modelling**

***Abstract*—The calculation of high-frequency winding losses caused by eddy currents in solid conductors with circular cross-section has already been discussed sufficiently often. However, there is currently no such treatment for conductors with rectangular cross-section in literature. In this article such a model is presented, which is based on a simplified two-dimensional formulation for the magnetic field inside conductors with rectangular cross-section. Similar to existing circular conductor models, the formulation is linked to an external, magneto-quasi-static field in the core window by means of boundary conditions, which makes it possible to a certain degree to calculate the frequency-dependent eddy current losses.**

I. INTRODUCTION

Rectangular conductors with larger cross-sections are typically considered when high DC currents (as part of the current spectrum) are present and a high copper fill factor is desired. Furthermore, tightly packed rectangular conductor windings offer better thermal properties. On the other hand, PCB windings consisting of conductors with rectangular cross-section simplify manufacturing. However, additional high-frequency components of the current spectrum induce high eddy current losses in rectangular conductors.

Typical loss calculation procedures combine the conductors with rectangular cross-section into equivalent foil layers of the same width (cf. figure 2), e.g. [1], [2], and calculate the resulting losses using known formulae for foil conductors [3]. In this approach, strictly axial fields must be assumed[1]. In order to satisfy the fact that not one solid foil conductor but several smaller solid conductors are considered, the conductivity must be modified with the so-called "porosity factor". The problem here is that the field between the conductors in radial direction is not taken into account, and furthermore, an inhomogeneous field along the axial direction of the equivalent foils cannot be taken into account (spatially inhomogeneous fields in axial direction occur for example in gapped devices, as depicted in figure 8). Hence, this procedure could result in severe errors that cannot be ignored [4],

[1]Throughout this paper, "axial" refers to the y-direction and "radial" refers to the x-component of a field, cf figure 1(a).

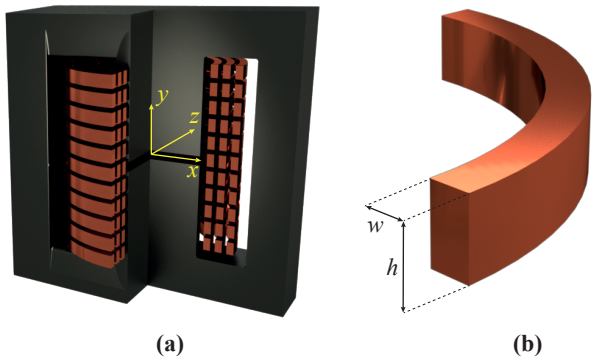

Fig. 1. Schematic of **(a)** an inductor with a winding made of conductors with rectangular cross-section and an air gap in the center leg, and **(b)** a conductor with rectangular cross-section, width w, and height h.

which was shown by a phenomenological study [5].

However, models that explicitly compute the power losses raised in a conductor with rectangular cross-section at high frequencies due to the current flow and an additional external magnetic field cannot be found in literature [6]. Only in [7], a greatly simplified formula for foil conductors is used for calculating the eddy currents in conductors with rectangular cross-section. In this approach it is assumed that the field can penetrate the conductor unhindered at any frequency. As shown in section III-B of this paper, this model leads to large errors when the conductor is larger than the skin depth at the respective frequency. In addition, [8] performs an analytical study of the skin effect. The presented model is limited by its symmetry assumption. [9] proposes a formally correct solution of the Maxwell equations based on Green's second identity, which is not considered in this context due to its complicated and computationally intensive nature[2].

In order to compute the eddy current losses raised in a conductor with rectangular cross-section, this paper presents a simplified analytical approach to model the high-frequency (HF) eddy current interactions in conductors with rectangular cross-section (as shown in figure 1 & 3). Although, as shown in section III, the proposed model does not predict the losses perfectly accurate, the general trend of the losses vs. frequency is modelled much better than with known models.The paper is structured as follows: Section II proposes the model in five steps, the following section III provides verification of the model and shows its limitations, and finally, section IV discusses the results.

II. Model

Typical state-of-the-art loss models for conductors with circular cross-section separate the problem of the field computation [10], [11] and the calculation of the losses caused by the magnetic field [12]. In order to use such approaches for conductors with rectangular cross-section, a model for the field inside the conductor is required, which can be linked to the external field by boundary conditions.

For this purpose, this section provides the derivation of such a model in five steps. First, the general assumptions are announced, followed by the presentation of the formulae for the magnetic field. Then, typical fields present in technical applications are discussed. Following this, the complex power, and finally a low-frequency (LF) variant of the formula is presented.

A. General assumptions

Inside the conductor (cf. figure 3) it is assumed that

1) all quantities are sinusoidal time-dependent with $\sin(\omega t + \phi)$, $\omega{=}2\pi f$, where the time-dependence is removed by means of the separation of variables,
2) it has a finite electrical conductivity $\sigma{\neq}0$,
3) it has a relative permeability $\mu_\mathrm{r}{=}1$,
4) electric field and current density are through-plane (only z-component), and the magnetic field is in-plane (x- and y-components).

B. Formulation of the 2D model

Generally, the magnetic field inside a conductive domain must satisfy the Helmholtz equation [12]

$$\nabla^2 \underline{\vec{H}} = \underline{\gamma}^2 \underline{\vec{H}} \tag{1}$$

with the propagation constant $\underline{\gamma}$ and the skin depth δ:

$$\gamma = {}^{1+\mathrm{i}}/_{\delta} \qquad \text{and} \qquad \delta = \sqrt{{}^{2}/_{\omega\sigma\mu_0}}.$$

The field components, which satisfy the Helmholtz equation (1) are proposed according to (2). This solution has the advantage compared to [8], that all four conductor

[2]Computations times in the range of FEM simulations must be expected.

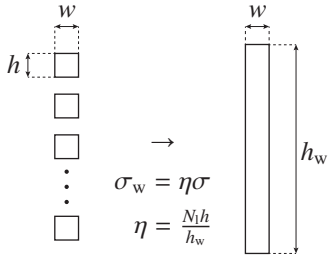

Fig. 2. Porosity factor to modify the conductivity σ_w of the equivalent foil conductor as proposed in [3] – N_l denotes the number of conductors per layer, h_w denotes the core window height.

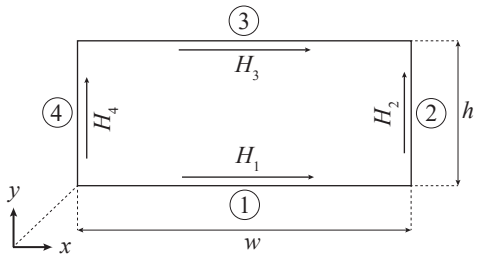

Fig. 3. Cross-section of a rectangular conductor with width w and height h – the local coordinate system is originated in the lower left corner of the conductor.

surfaces can have a distinct field value assigned to them (cf. figure 3).

$$\begin{aligned}\underline{H}_x &= \frac{H_1 \sinh\left(\underline{\gamma}\,(h-y)\right)}{\sinh\left(\underline{\gamma} h\right)} + \frac{H_3 \sinh\left(\underline{\gamma} y\right)}{\sinh\left(\underline{\gamma} h\right)} \\ \underline{H}_y &= \frac{H_4 \sinh\left(\underline{\gamma}\,(w-x)\right)}{\sinh\left(\underline{\gamma} w\right)} + \frac{H_2 \sinh\left(\underline{\gamma} x\right)}{\sinh\left(\underline{\gamma} w\right)}\end{aligned} \tag{2}$$

With Ampère's law and the conductivity, the electric field is given according to (3).

$$\underline{E}_z = \frac{1}{\sigma}\underline{J}_z = \frac{1}{\sigma}\left(\frac{\partial \underline{H}_y}{\partial x} - \frac{\partial \underline{H}_x}{\partial y}\right) \tag{3}$$

Eventually, with the electric and magnetic fields known, the losses can be computed using Poynting's theorem (cf. section II-D).

C. Technical application

In order to be able to use (2) meaningfully, boundary conditions must be defined in the form of the four tangential fields. This can be done analogously to the procedure for round conductors, given in [12]. A current flows through the conductor and an external magnetic field is present. Considered individually, the current in the conductor will create a magnetic field at high frequencies, which in turn will induce eddy currents. Due to this interaction, the current is pushed to the edge of the conductor with increasing frequency (inner skin effect). A changing external magnetic field also induces eddy currents, that are directed such that the magnetic field created by the induced eddy currents oppose the changes in the initial magnetic field (Lenz's law). These interactions lead again to current displacement in the conductor (induced skin effect[3]). Due to the linearity of Maxwell's equations, both effects can be considered separately and the fields can be superimposed.

If the conductor carries a current (with the amplitude I), it is exposed to the self-generated magnetic field $\vec{H}_{\mathrm{int}}$, with the intensity:

$$H_{\mathrm{int}} = \frac{I}{2w + 2h} \tag{4}$$

This is a simplification, since it is assumed that the field on the conductor's surface is spatially homogeneous. A formally correct calculation of the field can be derived from [9].

In addition to $\vec{H}_{\mathrm{int}}$, it is assumed that an external magnetic field $\vec{H}_{\mathrm{ext}}$ exists, which has x- and y-components. By assuming that the dimensions of the conductor are significantly smaller than the overall dimensions of the core window, it can be assumed that the external field is locally homogeneous on the edge of the conductor. This external field is responsible for the induced skin effect. The external fields are generally given as a vector field, from whose components the tangential field strength on the conductor contour can be calculated as follows:

$$\begin{aligned}H_{\mathrm{ext},x} &= |H_{\mathrm{ext}}(x,y)| \cos\left(\angle H_{\mathrm{ext}}(x,y)\right) \\ H_{\mathrm{ext},y} &= |H_{\mathrm{ext}}(x,y)| \sin\left(\angle H_{\mathrm{ext}}(x,y)\right)\end{aligned}$$

Hereby, the angle $\angle H_{\mathrm{ext}}(x,y)$ is the angle between the field vector and the x-axis in Cartesian coordinates (cf. figure 8).

The field generated by the current and the external field can be superimposed with respect to their effect on the conductor. Then, the four tangential fields on the surface are:

$$\begin{aligned}H_1 &= H_{\mathrm{int}} + H_{\mathrm{ext},x} \quad \wedge \quad H_3 = -H_{\mathrm{int}} + H_{\mathrm{ext},x} \\ H_2 &= H_{\mathrm{int}} + H_{\mathrm{ext},y} \quad \wedge \quad H_4 = -H_{\mathrm{int}} + H_{\mathrm{ext},y}\end{aligned} \tag{5}$$

In the following, all variables subscripted with $_{\mathrm{int}}$ denote the inner skin effect, and those subscripted with $_{\mathrm{ext}}$ the induced skin effect.

D. Complex power

The time-average complex power, considering the magnetic and electric field phasors, is given with Poynting's theorem according to (6).

$$\underline{S} = -\frac{1}{2}\oint_C \left(\vec{\underline{E}} \times \vec{\underline{H}}^*\right) \cdot \vec{n}\ \mathrm{d}s \tag{6}$$

By substituting (5) into (2), (2) into (3), and eventually (2) and (3) into (6), one obtains (7).

$$\begin{aligned}\underline{S} &= \underbrace{\frac{\underline{\phi}}{\sigma}\frac{I^2}{(2w+2h)^2}}_{\underline{S}_{\mathrm{int}}} + \underbrace{\frac{\underline{\psi}_x}{\sigma}H_{\mathrm{ext},x}^2 + \frac{\underline{\psi}_y}{\sigma}H_{\mathrm{ext},y}^2}_{\underline{S}_{\mathrm{ext}}} \\ \underline{\phi} &= \left(4 + \underline{\gamma} h \coth\left(\frac{\underline{\gamma} w}{2}\right) + \underline{\gamma} w \coth\left(\frac{\underline{\gamma} h}{2}\right)\right) \\ \underline{\psi}_x &= \underline{\gamma} w \tanh\left(\frac{\underline{\gamma} h}{2}\right) \quad \wedge \quad \underline{\psi}_y = \underline{\gamma} h \tanh\left(\frac{\underline{\gamma} w}{2}\right)\end{aligned} \tag{7}$$

It can observed that the impact of the inner and the induced skin effect are separated into $\underline{S}_{\mathrm{int}}$ and $\underline{S}_{\mathrm{ext}}$, as it is with comparable circular conductor models or known (1D) foil conductor models.

[3] If this field is generated by other conductors in close proximity, the effect is typically called "proximity effect".

E. Low frequency approximation

At low frequencies, which means *the largest dimension of the conductor is smaller than 1.6 times the penetration depth*, e.g., $d/\delta \leq 1.6$ [13, section 5.2.1], the magnetic field can penetrate the conductor approximately unperturbed by the induced eddy currents. For such cases, Taylor approximations of the components from (7) yield:

$$P_{\text{int}} = \frac{I^2}{\sigma w h}\left(\frac{1}{2} + \frac{\pi^2 f^2 \sigma^2 \mu_0^2 \left(w^4 h^2 + w^2 h^4\right)}{360\left(w+h\right)^2}\right) \qquad (8)$$

$$P_{\text{ext}} = \frac{\pi^2 f^2 \sigma \mu_0^2 w h}{6}\left(h^2 H_{\text{ext},x}^2 + w^2 H_{\text{ext},y}^2\right)$$

At higher frequencies (e.g., $d/\delta > 1.6$) these formulae result in large errors, because the approach does not take into account the repercussion of the induced eddy currents on the field generating them.

The above expression for P_{ext} is identical to [7, Eq. (10)], where the impact of the air gap fringing field on conductors with rectangular cross-section is investigated. The above expression for P_{int} was not found in literature. As shown in section III-A, this expression yields severe errors at frequencies above the threshold $d/\delta \leq 1.6$. For the sake of comparability, (8) is taken into consideration in this paper.

In all following sections, P_{int} and P_{ext} are used to denote the low-frequency (LF) approximation, whereas $\text{Re}(\underline{S}_{\text{int}})$ and $\text{Re}(\underline{S}_{\text{ext}})$ denote the losses computed with the proposed model.

III. Verification with FEM

In this section, the proposed 2D conductor model is compared to 2D FEM simulations in detail. The 2D FEM is used, because fully 3D models would create additional error sources (e.g., incorrect length scaling, field distortion at rounded corners of the winding, different core window geometries). In order to use the proposed model in a loss calculation procedure, appropriate length scaling of (7) must be applied.

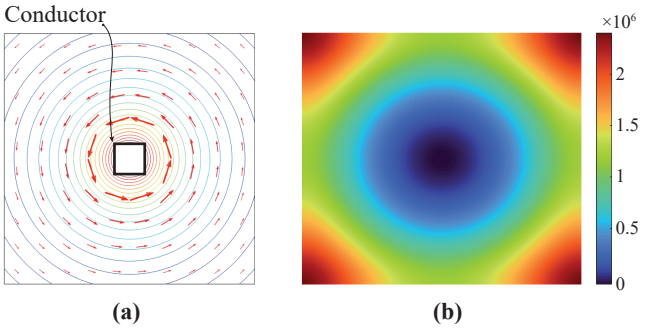

Fig. 4. Depiction of **(a)** a 1×1 mm conductor in its own magnetic field (arrows: magnetic vector field, lines: constant magnetic potential) and **(b)** the current density over conductor cross-section, computed with (3).

A. Inner skin effect

The inner skin effect, as described in section II-C, appears when a conductor carries a sinusoidal current with a specific frequency. This current generates a circular field around the conductor. In a rectangular conductor the field on the boundary is computed with the simplified approximation (4). For clarification, the case of a 1×1 mm conductor, carrying a current of 1 A at 100 kHz, is depicted in figure 4(a), and the resulting current density distribution inside the conductor is depicted in figure 4(b).

Furthermore, Figs. 5(a) and (b) provide the losses vs. the ratio of the (smallest) conductor dimension to the skin depth (in a range from 1 to 100), for the proposed model and the LF approximation (8), in comparison with a FEM simulation. It is shown, that the proposed model gives accurate results for $\text{Re}\{\underline{S}_{\text{int}}\}$ in a rectangular conductor, even for higher conductor-skin depth-ratios (cf. $w/\delta = 6.4$ in figure 5(b)). Hereby, the case of a square conductor is more accurate: The assumed magnetic field (4) deviates more from FEM for non-square conductors.

Errors obtained from the proposed model and the LF approximation in comparison to 2D FEM simulations are provided in table I.

B. Induced skin effect

A rectangular 2×1 mm conductor is placed in an external, spatially homogeneous magnetic field, where two cases are investigated:

1) radial field ($\angle H_{\text{ext}}(x,y) = 0$, cf. figure 6(a)),
2) mixed field ($\angle H_{\text{ext}}(x,y) = \pi/4$, cf. figure 6(b)),

both with intensity $|H_{\text{ext}}(x,y)| = 250$ A/m. The current density distribution, computed with the proposed formulae, is depicted in figure 6(c) and (d), respectively.

TABLE I
Errors obtained with the models compared to 2D FEM

Fig.	f (kHz)	Model	LF Appr.	h/δ	w/δ
5(a)	10	0 %	0 %	1.54	1.54
	100	-1 %	50 %	4.87	4.87
	1'000	-12 %	3'082 %	15.4	15.4
5(b)	10	-6 %	14 %	1.54	6.16
	100	-19 %	1'161 %	4.87	19.5
	1'000	-23 %	40'087 %	15.4	61.6

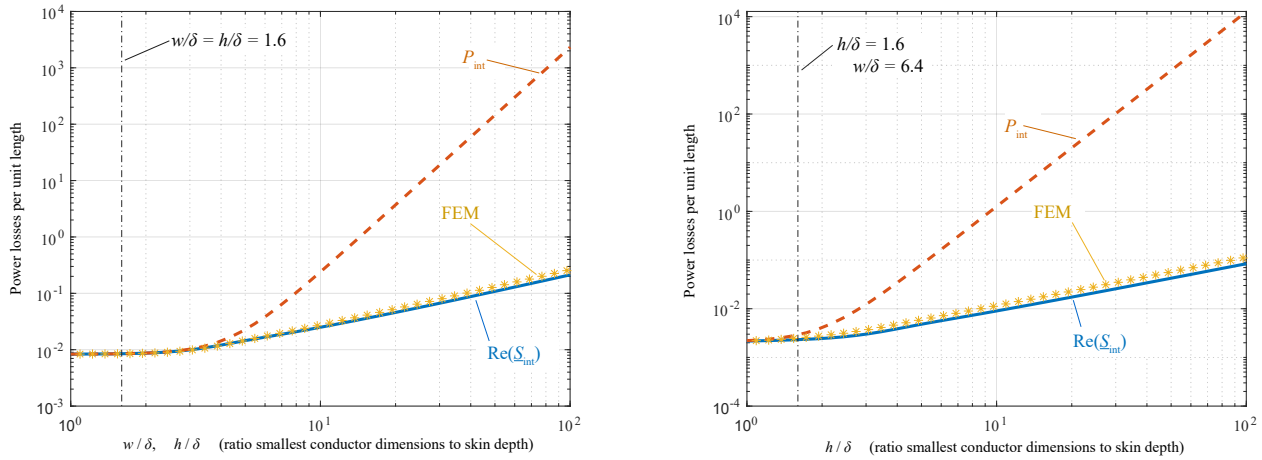

Fig. 5. Logarithmic plots of the power losses per unit length (vertical axis) vs. the relation of the smallest conductor dimension to the skin depth (horizontal axis). **(a)** Eddy current losses in a 1×1 mm conductor. **(b)** Eddy current losses in a 1×4 mm conductor.

Case 1) By inspection of the computed loss curves vs. h/δ (Figs. 7(a)), it can be observed that the proposed model and the LF approximation match well with FEM simulations for all conductor-skin depth-ratios up to 1.6 and even above, which is in accordance with the assumption from section II-E. The proposed model becomes identical to [3] in this case. At comparatively low frequencies, the conductor dimension perpendicular to the field dominates the losses, as it is known from [3]. However, when the internally generated field becomes noticable, the predicted losses $\mathrm{Re}\{\underline{S}_{\mathrm{ext}}\}$ underestimate the actual losses. The reason is, that the induced field also possesses a component in axial direction, which in turn generates eddy currents. This is is shown table II. The fields H_1 and H_4 (cf. figure 3) are extracted from the FEM simulation[4]. It can be observed, that at low frequencies, any field in axial direction (H_4) is neglectable, whereas at higher frequencies a non-neglectable field in axial direction is present, even though the external field has no such component. Furthermore, also the radial field component is strongly increased due to internal eddy current interactions. Generally, the proposed formula follows the results obtained with FEM simulations relatively good, whereas the LF approximation overestimates the losses quite substantially. However, the proposed model underestimates the losses, which might be problematic in terms of optimizations, since the real design would later exhibit higher losses than predicted and may overheat.

TABLE II
AVERAGE MAGNETIC FIELD STRENGTH ON THE CONDUCTOR SURFACES 1 AND 4 FOR VARYING FREQUENCIES

f (Hz)	H_1 (A/m)	H_4 (A/m)	h/δ
100	250	0	0.09
1'000	250	3	0.27
10'000	256	32	0.87
100'000	317	134	2.75
1'000'000	341	190	8.68

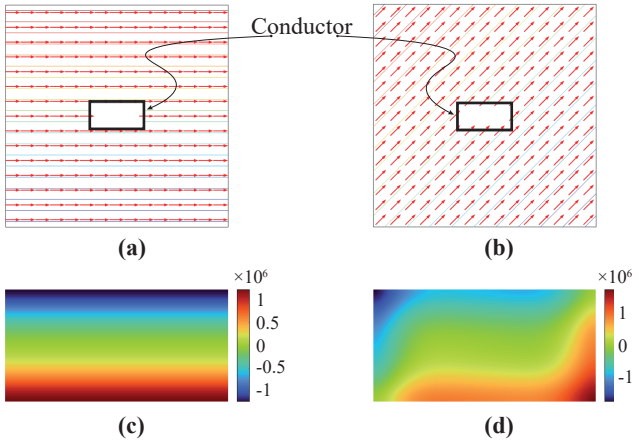

Fig. 6. Depiction of **(a)** a 2×1 mm conductor in an external, exclusively radial field, **(b)** a 2×1 mm conductor in an external, mixed radial and axial field (arrows: magnetic field vector, lines: constant magnetic potential), **(c)** the resulting current density of (a), and **(d)** the resulting current density of (b), both computed with (3) over the conductor cross-section.

[4]The spatial r.m.s. value along the respective surface is taken.

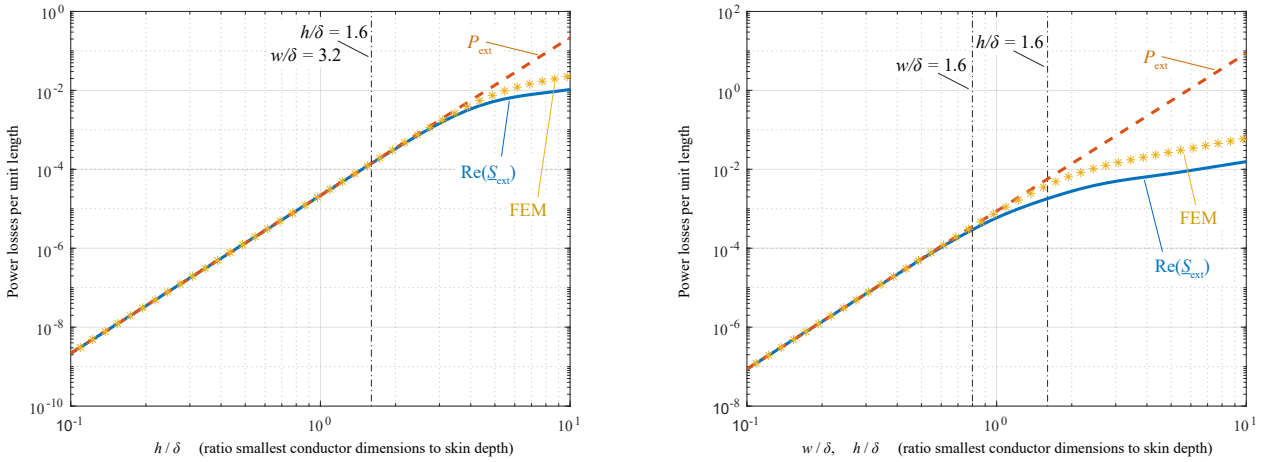

Fig. 7. Logarithmic plots of the power losses per unit length (vertical axis) vs. the relation of the smallest conductor dimension to the skin depth (horizontal axis). **(a)** Eddy current losses in a 1×2 mm conductor in a strictly radial field. **(b)** Eddy current losses in a 1×2 mm conductor in a mixed radial and axial field.

Case 2) Here, the field possesses both spatial components. By inspection of figure 7(b) it can be observed, that in this case the larger conductor dimension (radial dimension) w dominates the behaviour in terms of induced losses. This is true in general for arbitrary fields. Up to a ratio of $w/\delta = 1.6$, all models predict the same losses. At higher ratios, the proposed formulae tend to underestimate the losses. This is again due to the eddy current and field interactions, that lead to higher surface fields than assumed in the modelling approach. The LF approximation again overestimates the losses substantially and the proposed formulae follow the course of the FEM values relatively well, but underestimate the losses significantly. Table III provides errors at different frequencies for the scenarios shown in figure 7.

C. Winding example

Finally, the proposed model is applied in the context of a state-of-the-art analytical loss computation of magnetic devices. Since the formulae are supposed to model conductor losses caused by spatially inhomogeneous external fields, the device is assumed to be a gapped inductor, which has a single gap in the center leg (cf. figure 1) of length $l_\mathrm{g} = 2\,\mathrm{mm}$. The 2D model that is derived for this case is depicted in figure 8. The winding is assumed to consist of $N = 24$ conductors, each carrying a current $I = 1\,\mathrm{A}$, and the air gap is modelled as a current strip conducting a line current density $NI/l_\mathrm{g} = -12\,\mathrm{kA/m}$, as proposed in [14]. The magnetic field of such a current strip can be computed analytically [15]:

$$\begin{aligned} H_x &= \frac{K_z}{2\pi}\left(\ln\left(x^2+y_2^2\right) - \ln\left(x^2+y_1^2\right)\right) \\ H_y &= -\frac{K_z}{\pi}\left(\arctan\left(\frac{y_2}{x}\right) - \arctan\left(\frac{y_1}{x}\right)\right) \end{aligned} \tag{9}$$

In (9), $y_1 = y + l_\mathrm{g}/2$, $y_2 = y - l_\mathrm{g}/2$, $K_z = -NI/l_\mathrm{g}$, N is the number of conductors, and l_g is the air gap height (cf. figure 8). In order to use these field expressions in the considered case, the squared average of both field components of the fringing field (9) is computed numerically[5] in the region of interest (cf. figure 8 – "Area of integration"). To verify this approach, the comparison of the values obtained with values from a FEM simulation is given in table IV (for the purpose of this comparison, the respective area does not contain conductors that may perturbe the field).

The averaged squared field values are used to parametrize (7) and (8), and the total losses are obtained

TABLE III
ERRORS OBTAINED WITH THE MODELS COMPARED TO 2D FEM

Fig.	f (kHz)	Model	LF Appr.	h/δ	w/δ
7(a)	1	0 %	0 %	0.49	0.98
	10	-10 %	10 %	1.54	3.08
	100	-54 %	775 %	4.87	9.74
7(b)	1	-2 %	0 %	0.49	0.98
	10	-10 %	10 %	1.54	3.08
	100	-71 %	1739 %	4.87	9.74

[5] Analytical formulas for the calculation of the averaged squared fringing field can be found in [11].

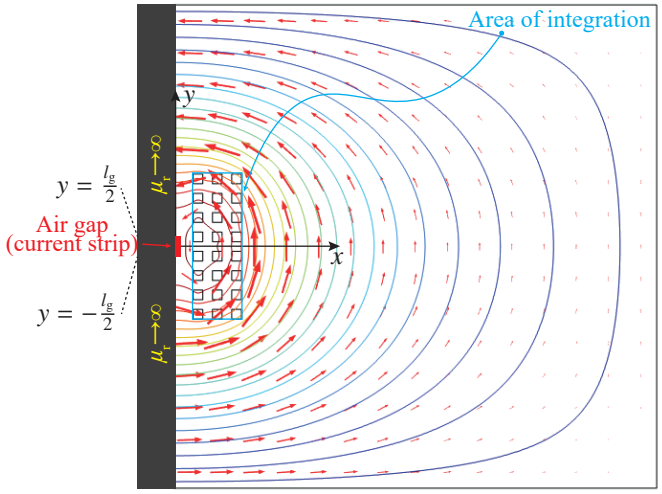

Fig. 8. Depiction of a winding in close vicinity to an air gap of length l_g (arrows: magnetic field vector, lines: constant magnetic potential).

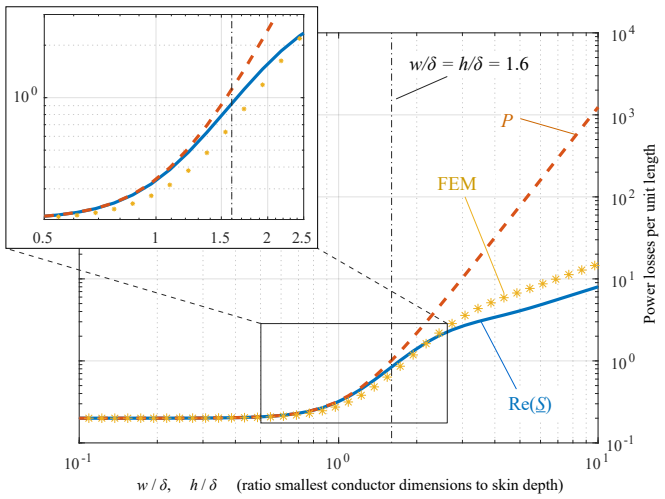

Fig. 9. Logarithmic plots of the power losses per unit length (vertical axis) vs. the relation of the smallest conductor dimension to the skin depth (horizontal axis): Eddy current losses in a winding in close vicinity to a current strip (the total losses with the LF approximation are $P = P_{\text{int}} + P_{\text{ext}}$).

TABLE IV
VERIFICATION OF THE ANALYTICAL FRINGING FIELD MODEL IN COMPARISON TO 2D FEM

	$H^2_{\text{ext},x}$ (A^2/m^2)	$H^2_{\text{ext},y}$ (A^2/m^2)
FEM	668'100	1'413'100
Num. int. of (9)	660'990	1'424'300
Rel. error* in %	-1.06	0.79

* $(H^2_{\text{num.int.}}/H^2_{\text{FEM}} - 1) \cdot 100\,\%$

by multiplication with the number of conductors. The comparison with a FEM simulation is shown in figure 9. In contrast to the expectation, that the proposed analytical model underestimates the losses in general, both analytical approaches overestimate the losses in the range $0.5 \leq h/\delta \leq 2.5$ (cf. figure 9, zoomed section). The reason can be found in the external magnetic field (9) that is applied to (7) and (8). FEM simulation results reveal, that in presence of the conductors with rectangular cross-section each carrying 1 A, the averaged field in the region of interest takes a different value. This is depicted in table V. As a consequence, the external field with less intensity induces less eddy currents, leading to the analytical models overestimating the losses. This is not visible at higher frequencies but is still present.

The results further reveal that the proposed model has the tendency to follow the FEM simulations well, but still underestimates the overall losses quite significantly for $h \geq 1.6\delta$, whereas the LF approximation, on the other hand, severly overestimates the total losses. This is expected from the results of the individual scenarios of the preceeding subsections. In order to verify the improved performance of the proposed formulae, table VI provides relative errors[6] of the models compared to FEM simulations.

IV. DISCUSSION OF THE RESULTS

Regarding the calculation of the inner skin effect losses, a slight underestimation of the losses is observed with the proposed model. The reason is, that the magnetic field (4) is assumed to be homogeneous along the

[6]Relative errors obtained with $(P_{\text{model}}/P_{\text{FEM}} - 1) \cdot 100\,\%$.

TABLE V
NUMERICAL EVALUATION OF THE AVERAGED SQUARED MAGNETIC FIELD IN THE "AREA OF INTEGRATION"

f (Hz)	$H^2_{\text{ext},x}$ (A^2/m^2)	$H^2_{\text{ext},y}$ (A^2/m^2)	h/δ
1	272'846	947'068	0.01
1'000	272'854	946'774	0.27
1'000'000	267'433	485'762	8.68

TABLE VI
ERRORS OBTAINED WITH THE MODELS COMPARED TO 2D FEM ACCORDING TO FIGURE 9

f (kHz)	Model	LF Appr.	h/δ	w/δ
1	2 %	2 %	0.49	0.49
10	32 %	55 %	1.54	1.54
100	-34 %	1066 %	4.87	4.87

surface, which in reality is not completely true. There, with increasing frequency, the field intensity would increase near the corners, which in turn leads to more increased local eddy currents, which causes a further increase in losses. However, the proposed expression is able to predict the additional losses due to the skin effect in a rectangular conductor quite accurately. The LF approximation P_{int} overestimates the losses by orders of magnitude, hence, (8) is not considered as an appropriate model for calculating the inner skin effect in conductors with rectangular cross-section.

From the findings given in section III-B, it can be concluded that a general model for conductors with rectangular cross-section must consider the eddy current interactions that lead to a coupled magnetic field inside the conductor. Then, both spatial components show dependencies in both spatial directions, hence,

$$\vec{H}(x,y) \stackrel{!}{=} \vec{e}_x H_x(x,y) + \vec{e}_y H_y(x,y)$$

which is not the case with (2). In addition, induced surface fields (cf. table II) must be considered in the modelling, which cannot be derived from the external field directly. Such a general model is proposed in [9] using Green's second identity, however, its computational burden is too high to be considered in terms of analytical loss computation in magnetic devices.

Eventually, section III-C reveals that with the proposed model it is qualitatively possible to estimate the increased eddy current losses in windings with rectangular conductors considering an inhomogeneous external field in the core window. The calculation results are more accurate than existing models [7].

Side note on the verification section: Note, that the proposed model is taylored to geometries where the external magnetic field is strongly inhomogeneous throughout the core window and may contain a radial field component (e.g., it may be a 2D field). This sets it apart from models using a strict 1D field assumption [1]–[3]. The only comparable model in literature is [7], which is identical to (8). Because 1D models are not suited to model the fringing field impact [4], the verification section does not compare those models to the proposed model. It can be argued that with existing models for round conductors [11] it would be possible to identify a rectangular conductor as an equivalent round conductor with the same cross section and use these models instead. However, as shown in section III-A of this paper, the current induced magnetic field and corresponding losses (e.g., skin losses) are captured quite well with the proposed approach. The larger error of the proposed model originates in the magnetic field distribution outside the conductors (cf. section III-B), that would be modelled incorrectly with all available models. A comparison of models to find the most suitable is not the topic of this paper.

V. Conclusion

In this paper, 2D magnetic field and winding loss models for conductors with rectangular cross-sections are proposed, phenomenologically studied, and results are presented for a range of geometrical aspect ratios and conductor dimension to skin depth ratios.

The results show, that the proposed model qualitatively reproduces the physical behaviour (simulated with 2D FEM simulations) of such a conductor, but the quantitative results show significant deviations from the benchmark results. In comparison to existing models, the presented approach offers much better accuracy, especially since high-frequency effects are considered more accurately.

References

[1] W. G. Hurley and W. H. Wölfle, *Transformers and Inductors for Power Electronics - Theory, Design and Applications*. John Wiley & Sons, Ltd, 2013.

[2] M. Kazimierczuk, *High Frequency Magnetic Components*. John Wiley & Sons, Ltd, 2013.

[3] P. L. Dowell, "Effects of eddy currents in transformer windings," in *Proc. of the Institution of Electrical Engineers*, vol. 113, no. 8, Aug. 1966, pp. 1387–1394.

[4] R. Prieto, J. Oliver, J. Cobos, J. Uceda, and M. Christini, "Errors obtained when 1d magnetic component models are not properly applied," in *APEC Fourteenth Annual Applied Power Electronics Conference and Exposition*, vol. 1. IEEE, 1999, pp. 206–212.

[5] F. Robert, P. Mathys, and J.-P. Schauwers, "The layer copper factor, although widely used and useful, has no theoretical base," in *31st Annual Power Electronics Specialists Conference*, vol. 3. IEEE, 2000, pp. 1633–1638.

[6] V. T. Morgan, "The current distribution, resistance and internal inductance of linear power system conductors - a review of explicit equations," *Transactions on Power Delivery*, vol. 28, no. 3, pp. 1252–1262, Jul. 2013.

[7] W. Roshen, "High-frequency fringing fields loss in thick rectangular and round wire windings," *IEEE Transactions on Magnetics*, vol. 44, no. 10, pp. 2396–2401, Oct. 2008.

[8] D. Gerling, "Approximate analytical calculation of the skin effect in rectangular wires," in *IEEE Int. Conf. on Electrical Machines and Systems (ICEMS)*, Nov. 2009.

[9] L. O. Fichte, "Berechnung der Stromverteilung in einem System rechteckiger Massivleiter bei Wechselstrom durch Kombination der Separations- mit der Randintegralgleichungsmethode," Ph.D. dissertation, Helmut-Schmidt-Universität, 2007.

[10] J. Muehlethaler, J. W. Kolar, and A. Ecklebe, "Loss modeling of inductive components employed in power electronic systems," in *8th Int. Conf. Power Electronics*, May 2011, pp. 945–952.

[11] T. Ewald and J. Biela, "Analytical winding loss and inductance models for gapped inductors with litz or solid wires," *IEEE Transactions on Power Electronics*, 2022.

[12] J. Lammeraner and M. Stafl, *Eddy currents*. Dorset House, Stamford Street, London: Lliffe Books Ltd., 1966.

[13] A. V. den Bossche and V. C. Valchev, "Improved calculation of winding losses in gapped inductors," *Journal of Applied Physics*, vol. 97, no. 10, May 2005.

[14] P. Wallmeier, N. Frohleke, and H. Grotstollen, "Improved analytical modeling of conductive losses in gapped high-frequency inductors," in *33rd Industry Applications Society Conf. (IAS)*, vol. 2. IEEE, Oct. 1998, pp. 913–920.

[15] H. A. Haus and J. R. Melcher, *Electromagnetic Fields and Energy*. Englewood Cliffs, New Jersey: Prentice Hall, 2008.